Article

Discovery Medicine 2026; 38(210): 2260–2270
https://doi.org/10.24976/Discov.Med.202638210.177

GCN2 Activation Promotes PD-L1 Expression and Survival of RPMI-8226 Multiple Myeloma Cells: An *In Vitro* Study Under Arginine Deprivation

Jing Peng[1], Yongqing Jia[1], Lina Zhang[2,*]

[1]Department of Hematology, Jinhua Municipal Central Hospital Medical Group, 321000 Jinhua, Zhejiang, China
[2]Department of Hematology, Wuxi Traditional Chinese Medicine Hospital, 214071 Wuxi, Jiangsu, China
*Correspondence: zln0525@163.com (Lina Zhang)
Submitted: 3 February 2026 Revised: 20 May 2026 Accepted: 10 June 2026 Published: 23 July 2026

Background: Multiple myeloma (MM) features metabolic stress along with immune evasion in the bone marrow microenvironment. This study aimed to clarify the role of general control nonderepressible 2 (GCN2) kinase signaling in regulating MM cell survival and programmed death-ligand 1 (PD-L1) expression under amino acid deficiency.

Methods: RPMI-8226 multiple myeloma cells were cultured under arginine-deprived conditions to mimic metabolic stress. Activation of the GCN2 signaling pathway and its downstream effectors (activating transcription factor 4 [ATF4], C/EBP homologous protein [CHOP]) was assessed by Western blotting. Cell viability and apoptosis were evaluated using Cell Counting Kit-8 (CCK-8) assays and Annexin V/PI flow cytometry. PD-L1 expression was measured using Western blotting, quantitative real-time PCR (qRT-PCR), and flow cytometry. Functional immune effects were further examined in a co-culture system with peripheral blood mononuclear cells (PBMCs). The role of GCN2 was validated using the selective inhibitor GCN2iB and the stress mimetic halofuginone.

Results: Arginine deprivation markedly activated the GCN2–ATF4–CHOP signaling axis in MM cells, promoting cell viability and suppressing apoptosis. In contrast, pharmacological inhibition of GCN2 with GCN2iB significantly reduced cell viability and increased apoptosis. GCN2 activation also upregulated PD-L1 expression at both transcriptional and surface levels, whereas GCN2 inhibition attenuated this effect. In a co-culture system, GCN2-mediated PD-L1 upregulation impaired T-cell activation, as evidenced by decreased CD69/CD25 expression and reduced IFN-γ secretion; these effects were partially reversed by GCN2 inhibition or PD-L1 blockade. Additionally, GCN2 inhibition exhibited limited cytotoxicity in PBMCs, indicating relative selectivity toward tumor cells. Halofuginone recapitulated the effects of amino acid deprivation, further confirming the role of GCN2 in metabolic and immunoregulatory adaptation.

Conclusion: GCN2 functions as a critical metabolic stress sensor in RPMI-8226 multiple myeloma cells, promoting tumor cell survival and immune evasion through PD-L1 upregulation under amino acid deprivation. Targeting the GCN2 pathway may represent a dual-acting therapeutic strategy to impair both metabolic adaptation and PD-L1 activation in MM.

Keywords: GCN2 kinase; multiple myeloma; amino acid deprivation; PD-L1; cell survival; apoptosis; immune evasion; stress response

Introduction

Multiple myeloma (MM) represents a hematologic cancer defined by clonal expansion of abnormal plasma cells within the bone marrow microenvironment [1]. Despite recent therapeutic improvements, MM remains difficult to cure, with frequent relapse and progression, particularly because of the complex interaction of tumor cell stress responses and immune evasion mechanisms [2]. The bone marrow niche is inherently hypoxic and nutrient-deprived, creating a stressful metabolic environment that promotes tumor adaptation and therapy resistance [3]. Among various stress-related adaptive responses, amino acid deprivation has emerged as a key modulator of cancer cell behavior, yet its specific contribution to MM pathophysiology remains underexplored.

Recent studies have highlighted the general control nonderepressible 2 (GCN2) kinase as a central sensor of amino acid scarcity, which initiates the integrated stress response (ISR) via phosphorylation of eukaryotic initiation factor 2 alpha (eIF2α) [4,5,6], leading to translational reprogramming and selective induction of adaptive transcriptional regulators such as activating transcription factor 4 (ATF4) and C/EBP homologous protein (CHOP) [7]. In several tumor types, GCN2 activation promotes cell survival under nutrient deprivation and enhances resistance to chemotherapy [8]. Notably, GCN2 has also been implicated in the upregulation of immune checkpoint proteins, such as IDO1, thereby contributing to immune escape [9]. However, these findings have not been thoroughly investigated in the context of MM, where both metabolic adapta-

Copyright: © 2026 The Author(s). Published by Discovery Medicine. This is an open access article under the CC BY 4.0 license.
Note: *Discovery Medicine* stays neutral with regard to jurisdictional claims in published maps and institutional affiliations.

tion and immune modulation are critical to disease progression [10].

Emerging evidence suggests a mechanistic link between nutrient-sensing pathways and immune evasion in the tumor microenvironment. In particular, accumulating evidence highlights the role of IDO-mediated tryptophan metabolism in shaping immune suppression within the tumor microenvironment. For example, IDO-driven tryptophan depletion impairs $CD8^+$ T-cell function and survival, and promotes $PD\text{-}1^+$ T-cell infiltration, partly through metabolic reprogramming of MDSCs and modulation of AMP-activated protein kinase (AMPK) activity in both suppressive and effector immune cells [11]. GCN2-dependent ATF4 signaling may serve as a key mediator linking mitochondrial ATP deficits to integrated stress response activation [12]. However, whether GCN2 plays a similar regulatory role in MM under amino acid stress remains unknown. Furthermore, the functional consequences of GCN2 inhibition on MM cell survival, apoptosis, and PD-L1 expression require further investigation to clarify its therapeutic relevance.

In this study, an *in vitro* amino acid deprivation model was established by culturing RPMI-8226 myeloma cells in arginine-free medium. GCN2 activation and its downstream effectors (ATF4 and CHOP) were assessed by Western blotting, and the selective inhibitor GCN2iB was used to evaluate its effects on cell viability, apoptosis, and programmed death-ligand 1 (PD-L1) expression. Halofuginone served as a pharmacologic mimic of amino acid stress. This work aimed to elucidate the function of GCN2 signaling in myeloma cell survival and PD-L1 regulation under nutrient deprivation, and to clarify its therapeutic relevance in both metabolic adaptation and immune evasion.

Materials and Methods

Cell Culture and Experimental Treatments

RPMI-8226 human multiple myeloma cells (Cell Bank of the Chinese Academy of Sciences, Shanghai, China, Cat# TCHu234) were used for all experiments. The cells were confirmed to be free of mycoplasma contamination and had been authenticated by short tandem repeat (STR) profiling according to the cell bank records. Cells were maintained in RPMI-1640 medium (MeilunBio, Dalian, China, Cat# PWL004) supplemented with 2 mM L-glutamine (Yujia, Guangzhou, China, Cat# C0212), 10% fetal bovine serum (FBS, ExCell Bio, Shanghai, China, Cat# FND500), and 1% penicillin–streptomycin (Yujia, Guangzhou, China, Cat# C0222) under standard conditions (37 °C, 5% CO_2). For arginine deprivation, cells were cultured in arginine-free RPMI-1640 medium (MeilunBio, Dalian, China, Cat# MA0546), supplemented with 10% dialyzed fetal bovine serum to simulate nutrient stress conditions relevant to the tumor microenvironment, particularly localized amino acid limitation. GCN2iB (TargetMol, Cat# T11375), a selective GCN2 inhibitor, was used for pharmacological inhibition of GCN2 signaling [13]. Halofuginone (Selleck Chemicals, Houston, TX, USA, Cat# S8144), a well-established activator of the amino acid starvation response and GCN2-mediated integrated stress response, was used to pharmacologically activate stress signaling [14].

Peripheral blood mononuclear cells (PBMCs) were purchased from Procell Life Science & Technology Co., Ltd. (Wuhan, China, Cat# CP-H158). PBMCs were derived from healthy donors and were confirmed to be free of mycoplasma contamination. PBMCs appeared predominantly round and exhibited a semi-adherent and semi-suspension growth pattern, consistent with the characteristics reported by the supplier. Cells were cultured in RPMI-1640 medium (MeilunBio, Dalian, China, Cat# PWL004) supplemented with 10% fetal bovine serum (FBS, ExCell Bio, Shanghai, China, Cat# FND500) and 1% penicillin–streptomycin (Yujia, Guangzhou, China, Cat# C0222) under standard conditions (37 °C, 5% CO_2) and used for subsequent co-culture experiments.

For arginine-deprivation model establishment and GCN2iB dose-response analyses, the following treatment groups were established. The Control group was maintained in complete RPMI-1640 medium, whereas the Arg– group was cultured in arginine-free RPMI-1640 medium supplemented with 10% dialyzed FBS. To examine early activation of the GCN2 pathway, RPMI-8226 cells were exposed to arginine deprivation for 6 h or 24 h, followed by Western blot analysis of p-GCN2, total GCN2, ATF4, and CHOP. For GCN2iB dose-response experiments, arginine-deprived RPMI-8226 cells were treated with GCN2iB at final concentrations of 0.5, 1, 2, or 5 μM. Western blot analysis of GCN2 pathway proteins was performed after 24 h of treatment, cell viability was measured at 24, 48, and 72 h, and apoptosis was assessed after 48 h. Based on these dose-response results, 2 μM GCN2iB was selected for subsequent mechanistic experiments.

For bidirectional modulation and PD-L1 expression analyses, RPMI-8226 cells were assigned to four groups: Control, Arg–, Arg– + GCN2iB (2 μM), and halofuginone (50 nM) [15]. Halofuginone was administered in complete RPMI-1640 medium for 24 h to pharmacologically mimic amino acid starvation-related stress signaling. After 24 h of treatment, GCN2 pathway proteins, apoptosis-related proteins, and PD-L1 expression were assessed by Western blotting, qRT-PCR, and/or flow cytometry, as appropriate. Cell viability under these conditions was evaluated using CCK-8 assays at 24, 48, and 72 h.

For co-culture experiments, RPMI-8226 cells were first pretreated under Co-Ctrl, Co-Arg–, or Co-Arg– + GCN2iB (2 μM) conditions for 24 h. After pretreatment, the culture supernatant was discarded, and the cells were gently washed with PBS to remove residual treatment reagents. The pretreated RPMI-8226 cells were then resuspended in fresh complete co-culture medium and co-

cultured with PBMCs for 48 h. In the PD-L1 blockade group, RPMI-8226 cells were first pretreated with arginine-free medium for 24 h, washed with PBS, and then co-cultured with PBMCs in fresh complete medium containing an anti-human PD-L1 neutralizing antibody at a final concentration of 5 μg/mL for 48 h [16]. After co-culture, PBMCs were collected for flow-cytometric analysis of $CD3^+CD69^+$ and $CD3^+CD25^+$ T-cells, and culture supernatants were harvested for IFN-γ detection by ELISA. To evaluate the relative selectivity of GCN2 inhibition, PBMCs under arginine-deprived conditions were treated with GCN2iB at 0.5, 1, 2, or 5 μM; apoptosis was assessed after 48 h, and cell viability was measured at 24, 48, and 72 h.

Western Blotting

Total protein was extracted using RIPA buffer (Beyotime, Shanghai, China) supplemented with protease and phosphatase inhibitors (Thermo Fisher Scientific, Waltham, MA, USA, Cat# 78440), and concentrations were determined using a BCA Protein Assay Kit (Beyotime, Shanghai, China, Cat# P0009). Protein aliquots (30–50 μg) were subjected to SDS-PAGE, transferred onto PVDF membranes (Millipore, Billerica, MA, USA, Cat# FFP24), and incubated in 5% non-fat milk for 1 h at room temperature.

Overnight incubation at 4 ℃ was performed using primary antibodies against p-GCN2 (Thr899 phosphorylation site, Abcam, Cambridge, UK, Cat# ab75836, rabbit, 1:1000), GCN2 (Abcam, Cambridge, UK, Cat# ab134053, rabbit, 1:1000), ATF4 (Abcam, Cambridge, UK, Cat# ab216839, rabbit, 1:1000), CHOP (Abcam, Cambridge, UK, Cat# ab11419, mouse, 1:1000), Bcl-2 (Abcam, Cambridge, UK, Cat# ab182858, rabbit, 1:1000), Bax (Abcam, Cambridge, UK, Cat# ab32503, rabbit, 1:1000), PD-L1 (Abcam, Cambridge, UK, Cat# ab205921, rabbit, 1:1000), and β-actin (Abcam, Cambridge, UK, Cat# ab8226, mouse, 1:5000).

Membranes were washed and then incubated for 1 h at room temperature with HRP-conjugated secondary antibodies (goat anti-rabbit IgG, BIOSS, Beijing, China, Cat# bs-0295G-HRP, 1:5000; goat anti-mouse IgG, BIOSS, Beijing, China, Cat# bs-0296G-HRP, 1:5000). Signals were visualized using an enhanced chemiluminescence reagent (Millipore, Billerica, MA, USA, Cat# P0018S) and captured with the ChemiDoc XRS+ imaging system (Bio-Rad, Hercules, CA, USA). Band intensities were analyzed using ImageJ software (version 1.53, NIH, Bethesda, MD, USA), normalized to β-actin, and each experiment was independently performed in triplicate.

CCK-8 Cell Viability Assay

Cell viability was assessed using a Cell Counting Kit-8 (CCK-8; Beyotime, Shanghai, China, Cat# C0038). RPMI-8226 cells or PBMCs were seeded into 96-well plates (Jett Biofil, Guangzhou, China) at 1×10^4 cells per well in 100 μL medium. RPMI-8226 cells were treated under Control, Arg–, Arg– + GCN2iB (0.5–5 μM), or halofuginone (50 nM) conditions, whereas PBMCs were treated under Arg– conditions with or without GCN2iB (0.5–5 μM). At 24, 48, and 72 h after treatment, 10 μL of CCK-8 reagent was added to each well, followed by incubation for 2 h at 37 ℃. Absorbance was measured at 450 nm using a microplate reader (Synergy HTX, BioTek, Winooski, VT, USA). After subtraction of blank-well absorbance, relative cell viability was calculated as follows: cell viability (%) = [(A(treatment at each time point) − A(blank)) / (A(treatment at 0 h) − A(blank))] × 100.

Flow Cytometry

Flow cytometry was used to assess apoptosis and T-cell activation in the corresponding experimental settings. For apoptosis analysis, RPMI-8226 cells or PBMCs were collected after the indicated treatments. In the GCN2iB dose-response experiments, cells were treated under arginine-deprived conditions with or without different concentrations of GCN2iB for 48 h. For comparison among the Control, Arg–, Arg– + GCN2iB, and halofuginone groups, RPMI-8226 cells were collected after the corresponding treatments. Cells were stained with an Annexin V-FITC/PI Apoptosis Detection Kit (Beyotime, Shanghai, China, Cat# C1062) for 15 min at room temperature in the dark. Early and late apoptotic cells were defined as Annexin V^+/PI^- and Annexin V^+/PI^+ cells, respectively.

For PD-L1 surface expression analysis, RPMI-8226 cells were treated under Control, Arg–, Arg– + GCN2iB, or halofuginone conditions for 24 h, followed by staining with FITC anti-human CD38 antibody (BioLegend, San Diego, CA, USA, Cat# 303504) and PE anti-human CD274/B7-H1/PD-L1 antibody (BioLegend, Cat# 374512) for 30 min at 4 °C in the dark.

For T-cell activation analysis, PBMCs were collected after 48 h of co-culture and stained with APC anti-human CD3 antibody (BioLegend, Cat# 300412), PE anti-human CD69 antibody (BioLegend, Cat# 310906), and FITC anti-human CD25 antibody (BioLegend, Cat# 302604) for 30 min at 4 °C in the dark. T-cells were gated as $CD3^+$ cells, and activation was evaluated based on the proportions of $CD3^+CD69^+$ and $CD3^+CD25^+$ cells. All samples were analyzed using a BD FACSCanto™ II flow cytometer (BD Biosciences, San Jose, CA, USA), and data were processed using FlowJo software (version 10.0; BD Biosciences, Ashland, OR, USA).

Quantitative Real-Time PCR (qRT-PCR)

RNA extraction was performed using TRIzol reagent (Invitrogen, Thermo Fisher Scientific, Waltham, MA, USA), and purity was confirmed by an A260/280 ratio ranging from 1.8 to 2.0. RNA (2 μL) was used in one-step qRT-PCR reactions with the UniPeak U+ One Step SYBR Green Kit (TransGen Biotech, Beijing, China) on a real-

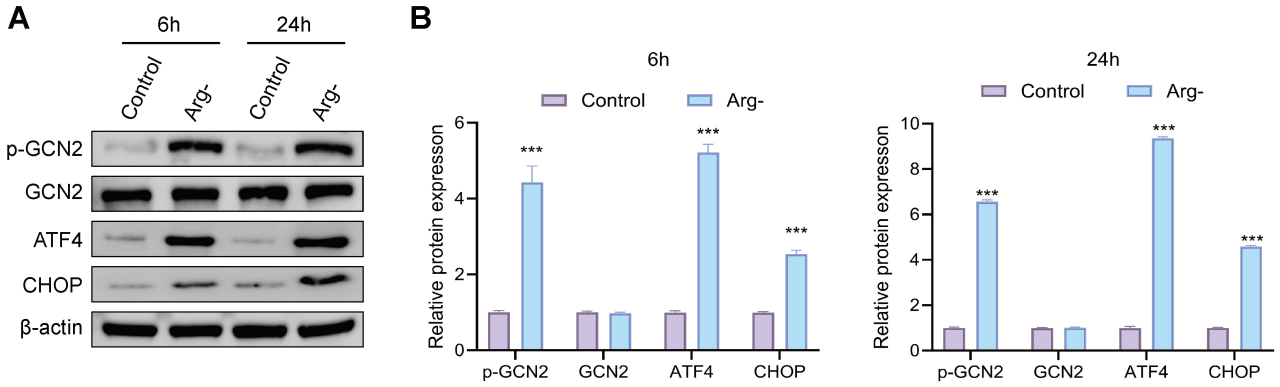

Fig. 1. Arginine deprivation activates the GCN2 stress signaling pathway in RPMI-8226 MM cells. (A) Representative Western blot results illustrating expression of GCN2 phosphorylation (p-GCN2), total GCN2, ATF4, and CHOP in cells treated under control conditions or arginine deprivation (Arg–) for 6 or 24 h. (B) Quantitative densitometry of protein expression levels at 6 h and 24 h. Data are presented as mean ± SD from three independent biological replicates. ***$p < 0.001$ vs Control group. GCN2, general control nonderepressible 2; MM, multiple myeloma; ATF4, activating transcription factor 4; CHOP, C/EBP homologous protein.

Table 1. Primer sequences used for quantitative real-time PCR analysis.

Gene	Primer name	Sequence (5′-3′)	Tm (°C)	Length (bp)
PD-L1	*PD-L1*-F	TGAACTGACATGTCAGGCTG	58.1	20
	PD-L1-R	CCAGAATTACCAAGTGAGTCC	58.4	21
GAPDH	*GAPDH*-F	AAGATCATCAGCAATGCCTCC	58.4	21
	GAPDH-R	AGGTTTTTCTAGACGGCAGG	58.1	20

The $2^{-\Delta\Delta Ct}$ method was employed to quantify relative gene expression, with GAPDH serving as the internal control. Triplicate reactions were performed, with no-template controls incorporated to confirm the absence of contamination. PD-L1, programmed death-ligand 1; GAPDH, glyceraldehyde-3-phosphate dehydrogenase.

time PCR system (QuantStudio 5, Thermo Fisher Scientific, Waltham, MA, USA) with a 20 µL reaction mixture comprising 10 µL Master Mix, 0.4 µL primers (10 µM each), and 7.2 µL RNase-free water. Cycling parameters included 55 ℃ for reverse transcription, 95 ℃ for initial denaturation, followed by 40 cycles of 95 ℃ denaturation and 60 ℃ annealing/extension, and melting curve analysis was automatically performed. Primer sequences are shown in Table 1, and amplification efficiency was confirmed to be 90–110% by standard curve analysis. Relative gene expression was calculated using the $2^{-\Delta\Delta Ct}$ method with *GAPDH* as the internal control. All reactions were performed in triplicate, and no-template controls were included to exclude contamination.

ELISA for Cytokine Detection

The levels of IFN-γ in the co-culture supernatants were measured using a human IFN-γ ELISA kit (Beyotime, China; Cat# PI511) according to the manufacturer's instructions. Absorbance was measured at 450 nm using a microplate reader, and cytokine concentrations were calculated based on standard curves.

Statistical Analysis

All experiments were performed with at least three independent biological replicates, and results are presented as mean ± SD. Statistical analysis was conducted using GraphPad Prism 9.0 (GraphPad Software, San Diego, CA, USA). The Shapiro–Wilk test was applied to assess normality, and Levene's test was used to evaluate homogeneity of variance. Two-group comparisons were performed using the unpaired two-tailed Student's *t*-test, whereas multiple group comparisons were conducted using one-way ANOVA followed by Tukey's post hoc test. Statistical significance was defined as $p < 0.05$.

Results

Arginine Deprivation Activates the GCN2-ATF4 Stress Signaling Pathway in MM Cells

To determine whether amino acid deprivation activates the GCN2 signaling pathway in multiple myeloma cells, RPMI-8226 cells were cultured under arginine-deprived conditions for 6 h and 24 h. Western blot analysis revealed that phosphorylation of GCN2 (p-GCN2) was markedly increased under arginine deprivation, whereas total GCN2 levels remained unchanged, indicating that the

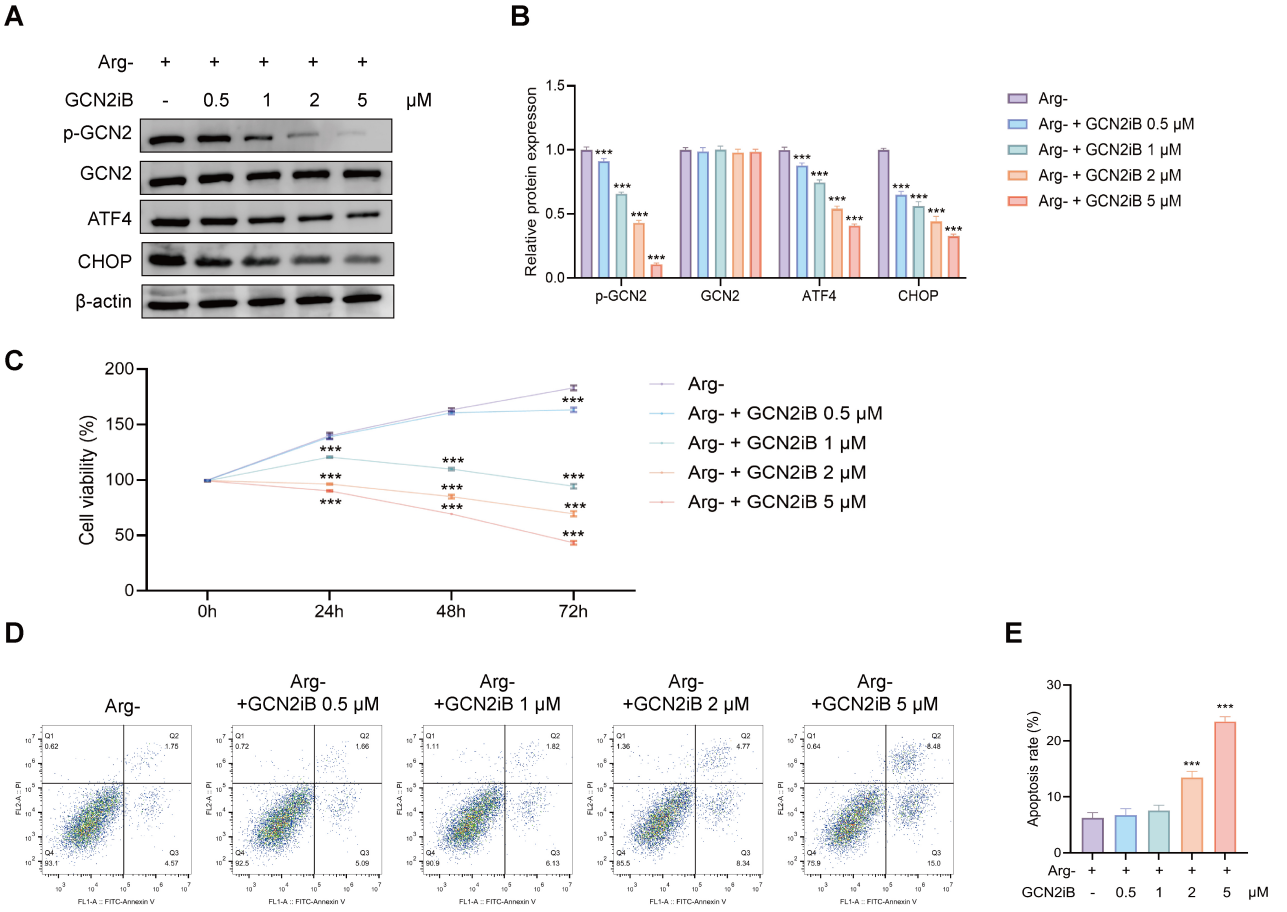

Fig. 2. GCN2 inhibition suppresses stress signaling, reduces viability and promotes apoptosis of MM cells under arginine deprivation. (A) Representative Western blot images showing the expression levels of p-GCN2, total GCN2, ATF4, and CHOP in RPMI-8226 cells cultured under arginine-deprived conditions (Arg–) and treated with increasing concentrations of GCN2iB (0.5, 1, 2, and 5 μM) for 24 h. (B) Quantification of protein expression levels. (C) CCK-8 assay showing the relative cell viability at 24 h, 48 h, and 72 h after GCN2iB treatment under arginine deprivation. (D) Representative flow cytometry plots of apoptosis in RPMI-8226 cells treated with increasing concentrations of GCN2iB under arginine deprivation for 48 h. Apoptosis was analyzed using Annexin V-FITC/PI staining. (E) Quantification of apoptotic cells based on flow cytometry analysis. Data are presented as mean ± SD from three independent biological replicates. ***$p < 0.001$ vs Arg– group. GCN2iB, GCN2 inhibitor B; CCK-8, Cell Counting Kit-8; V-FITC/PI, Annexin V-fluorescein isothiocyanate/propidium iodide; SD, standard deviation.

response was activation-dependent rather than expression-driven (Fig. 1A). The downstream stress-related transcription factors ATF4 and CHOP were also elevated at both 6 h and 24 h, with a further increase observed over time. Quantitative densitometry further confirmed that p-GCN2, ATF4, and CHOP levels were markedly increased at 24 h compared with the control group (Fig. 1B; $p < 0.001$). These findings demonstrate that arginine deprivation robustly activates the GCN2–ATF4–CHOP signaling axis in multiple myeloma cells.

Dose-Dependent Inhibition of GCN2 Suppresses Stress Signaling and Impairs MM Cell Survival

To evaluate the functional role of GCN2 under amino acid stress, RPMI-8226 cells were cultured in arginine-free medium with increasing concentrations of GCN2iB (0.5–5 μM) for 24 h. Western blot analysis demonstrated a dose-dependent reduction in p-GCN2, ATF4, and CHOP expression across the GCN2iB treatment groups (0.5, 1, 2, and 5 μM), while total GCN2 levels remained unchanged (Fig. 2A,B; $p < 0.001$). In parallel, CCK-8 assays showed that, compared with the Arg– group, cell viability progressively declined over time (24, 48, and 72 h) and was further reduced with increasing concentrations of GCN2iB, with more pronounced inhibitory effects observed in the higher-dose groups (Fig. 2C; $p < 0.001$). Consistently, flow cytometry analysis revealed a gradual increase in apoptotic cell populations across the GCN2iB-treated groups, with apoptosis being modest at lower concentrations and markedly elevated at higher concentrations under arginine-

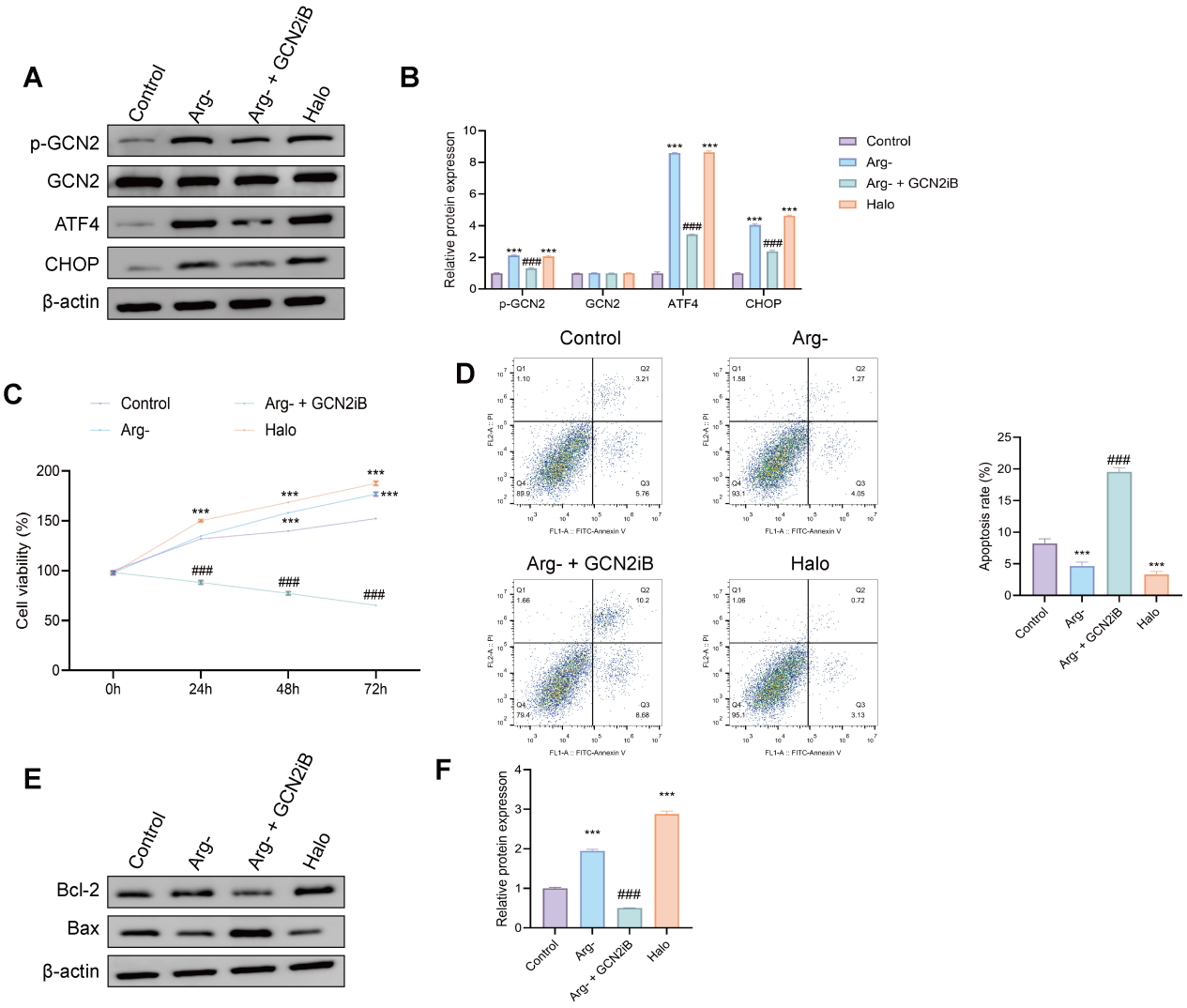

Fig. 3. GCN2 activation promotes MM cell survival and inhibits apoptosis under amino acid deprivation. (A) Representative Western blot images showing the expression of p-GCN2, total GCN2, ATF4, and CHOP in RPMI-8226 cells under Control, arginine deprivation (Arg–), Arg– + GCN2iB (2 μM), and Halofuginone (50 nM) conditions after 24 h. (B) Quantification of protein levels. (C) CCK-8 assay results showing cell viability at 24 h, 48 h, and 72 h under the four treatment conditions. (D) Apoptosis detected by flow cytometry using Annexin V-FITC/PI staining. (E) Expression of apoptosis-related proteins Bcl-2 and Bax analyzed by Western blotting under the same conditions. (F) Quantification of the Bcl-2/Bax ratio. Data are presented as mean ± SD from three independent biological replicates. ***$p < 0.001$ vs. Control group. $^{###}p < 0.001$ vs. Arg–group.

deprived conditions (Fig. 2D,E; $p < 0.001$). These findings demonstrate that GCN2 activity is required for maintaining MM cell survival under metabolic stress in a dose-dependent manner. Based on these dose–response results, 2 μM GCN2iB was selected for subsequent experiments, as it produced a clear inhibitory effect on GCN2 signaling and cell viability while avoiding excessive cytotoxicity observed at higher concentrations.

Bidirectional Modulation of GCN2 Confirms Its Role in MM Cell Survival and Apoptosis

To further validate the functional role of GCN2 beyond dose-dependent inhibition, RPMI-8226 cells were subjected to bidirectional modulation under Control, Arg–, Arg– + GCN2iB (2 μM), or halofuginone (50 nM) conditions. Western blot analysis showed that both arginine deprivation and halofuginone activated the GCN2–ATF4–CHOP signaling axis. Under arginine-deprived conditions, GCN2iB suppressed GCN2 pathway activation, as indicated by reduced p-GCN2, ATF4, and CHOP levels (Fig. 3A,B; $p < 0.001$). Functionally, arginine deprivation and halofuginone were associated with enhanced cellular viability and reduced apoptosis, likely reflecting adaptive responses under stress conditions. Under arginine-deprived conditions, GCN2iB reduced cell viability and increased apoptosis compared with the Arg– group (Fig. 3C,D; p

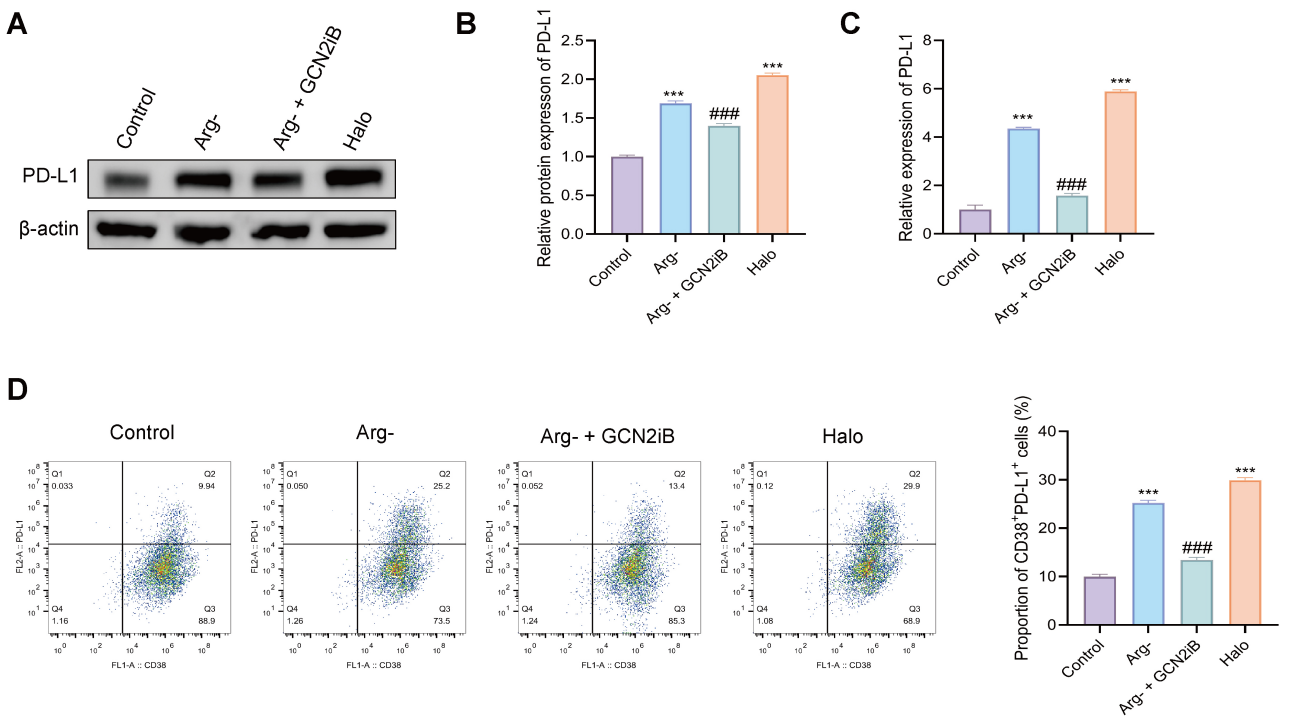

Fig. 4. GCN2 activation enhances PD-L1 expression in MM cells at the protein, transcriptional, and surface levels. (A) Representative Western blot images of PD-L1 protein expression in RPMI-8226 cells under Control, arginine deprivation (Arg–), Arg– + GCN2iB (2 μM), and Halofuginone (50 nM) treatments for 24 h. β-actin served as the loading control. (B) Quantitative densitometry of PD-L1 protein levels. (C) Relative mRNA expression levels of *PD-L1* measured by qRT-PCR under the same treatment conditions. (D) Representative flow cytometry dot plots showing $CD38^{+}PD\text{-}L1^{+}$ cells in each group, and quantification of the percentage of $CD38^{+}PD\text{-}L1^{+}$ cells (Q2 region) based on flow cytometry analysis. Data are presented as mean ± SD from three independent biological replicates. ***$p < 0.001$ vs. Control group. $^{###}p < 0.001$ vs. Arg–group.

< 0.001). Consistently, analysis of apoptosis-related proteins showed that arginine deprivation and halofuginone increased the Bcl-2/Bax ratio, indicating an anti-apoptotic shift. Under arginine-deprived conditions, GCN2iB reduced the Bcl-2/Bax ratio compared with the Arg– group (Fig. 3E,F; $p < 0.001$).

Collectively, these findings provide mechanistic evidence that GCN2 promotes MM cell survival by regulating apoptosis-related pathways under amino acid deprivation.

GCN2 Signaling Enhances PD-L1 Expression in MM Cells

To determine whether GCN2 activation regulates PD-L1 expression under amino acid deprivation, we examined PD-L1 at both protein and mRNA levels. Western blot analysis showed that PD-L1 protein expression was elevated in both the Arg– and halofuginone groups compared with the Control group. Under arginine-deprived conditions, GCN2iB partially reduced Arg—induced PD-L1 upregulation (Fig. 4A,B; $p < 0.001$). Consistently, qRT-PCR analysis revealed that *PD-L1* mRNA levels were significantly increased in the Arg– and halofuginone groups, with a reduction observed upon GCN2 inhibition (Fig. 4C; $p < 0.001$). Flow cytometry further demonstrated that the proportion of $CD38^{+}PD\text{-}L1^{+}$ cells was markedly increased under arginine deprivation and further enhanced by halofuginone, while treatment with GCN2iB led to a noticeable decrease compared with the Arg– group (Fig. 4D; $p < 0.001$).

These findings indicate that arginine deprivation and halofuginone are associated with increased PD-L1 expression, while pharmacological inhibition of GCN2 attenuates Arg—induced PD-L1 upregulation.

GCN2-Mediated PD-L1 Upregulation Suppresses T-cell Activation in a Co-Culture System

To further investigate the functional impact of GCN2-mediated PD-L1 upregulation on immune cell activity, RPMI-8226 cells pretreated under different conditions were co-cultured with PBMCs. Flow cytometry analysis showed that arginine deprivation significantly reduced the proportions of activated T-cells, as indicated by decreased percentages of $CD3^{+}CD69^{+}$ and $CD3^{+}CD25^{+}$ cells compared with the control group (Fig. 5A,B, $p < 0.001$). Notably, inhibition of GCN2 by GCN2iB partially restored T-cell activation, whereas blockade of PD-L1 using a neutralizing antibody led to a more pronounced recovery, approaching

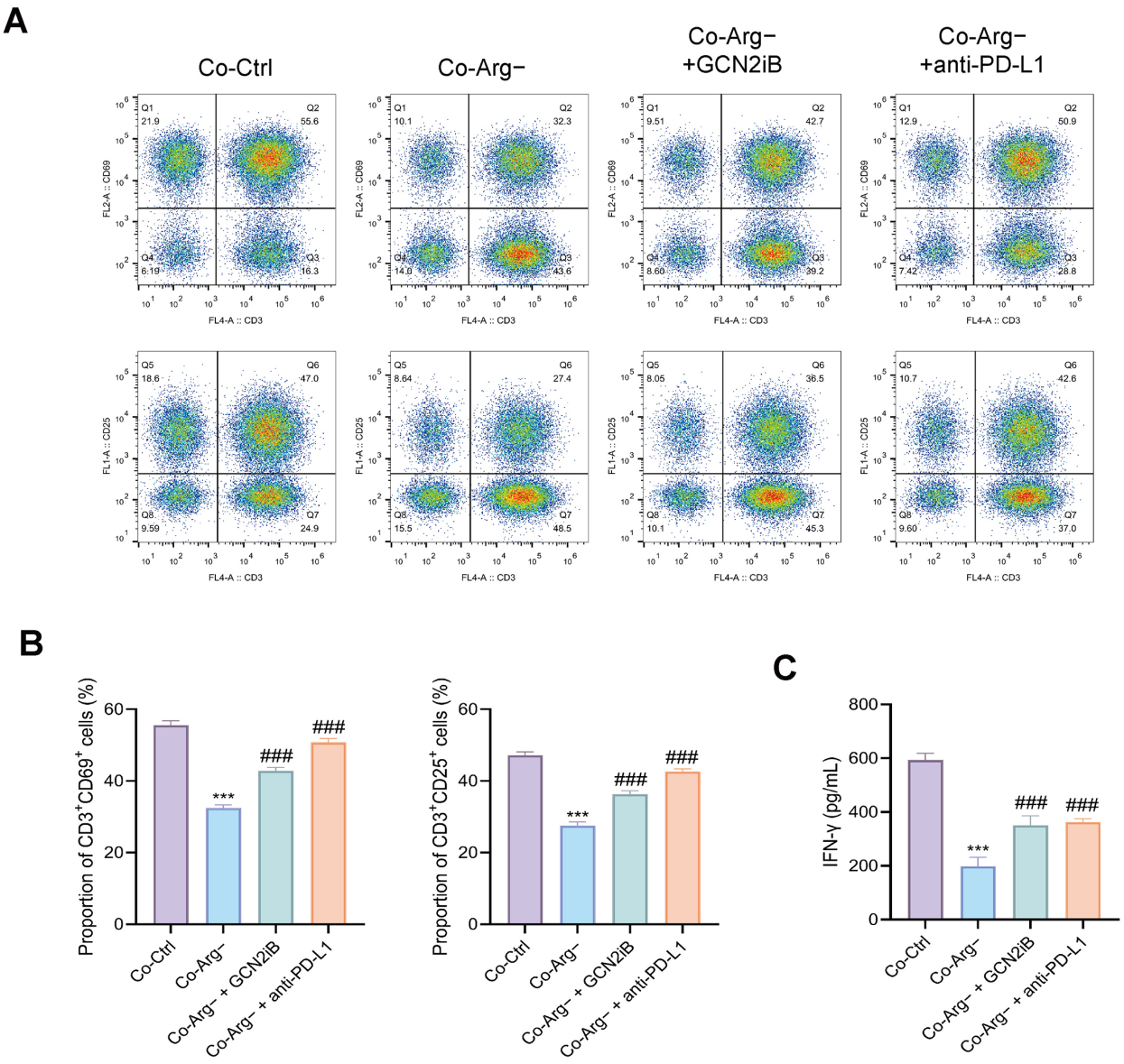

Fig. 5. GCN2-mediated PD-L1 upregulation suppresses T-cell activation in a co-culture system. (A) Representative flow cytometry plots showing the proportions of activated T-cells ($CD3^+CD69^+$ and $CD3^+CD25^+$) in PBMCs co-cultured with RPMI-8226 cells pretreated under different conditions: control (Co-Ctrl), arginine deprivation (Co-Arg–), arginine deprivation with GCN2 inhibition (Co-Arg– + GCN2iB, 2 μM), and arginine deprivation with PD-L1 blockade (Co-Arg– + anti-PD-L1). (B) Quantitative analysis of the proportions of $CD3^+CD69^+$ and $CD3^+CD25^+$ T-cells in each group based on flow cytometry data. (C) ELISA analysis of IFN-γ levels in culture supernatants of the co-culture system under the indicated conditions. Data are presented as mean ± SD from three independent biological replicates. ***$p < 0.001$ vs. Co-Ctrl group; $^{###}p < 0.001$ vs. Co-Arg– group. PBMCs, peripheral blood mononuclear cells; ELISA, enzyme-linked immunosorbent assay; IFN-γ, interferon-gamma.

control levels (Fig. 5A,B, $p < 0.001$). These results suggest that Arg—induced immunosuppression is, at least in part, mediated through the GCN2–PD-L1 axis.

Consistently, ELISA analysis demonstrated that IFN-γ secretion was significantly decreased in the Arg– group, while both GCN2 inhibition and PD-L1 blockade markedly increased IFN-γ levels in the co-culture system (Fig. 5C, $p < 0.001$). Together, these findings indicate that GCN2 activation promotes PD-L1-dependent immune suppression, thereby impairing T-cell activation under amino acid deprivation.

GCN2 Inhibition Exhibits Limited Cytotoxicity in PBMCs and Highlights Its Relative Selectivity

To evaluate the potential cytotoxic effects of GCN2 inhibition on normal immune cells, PBMCs were treated

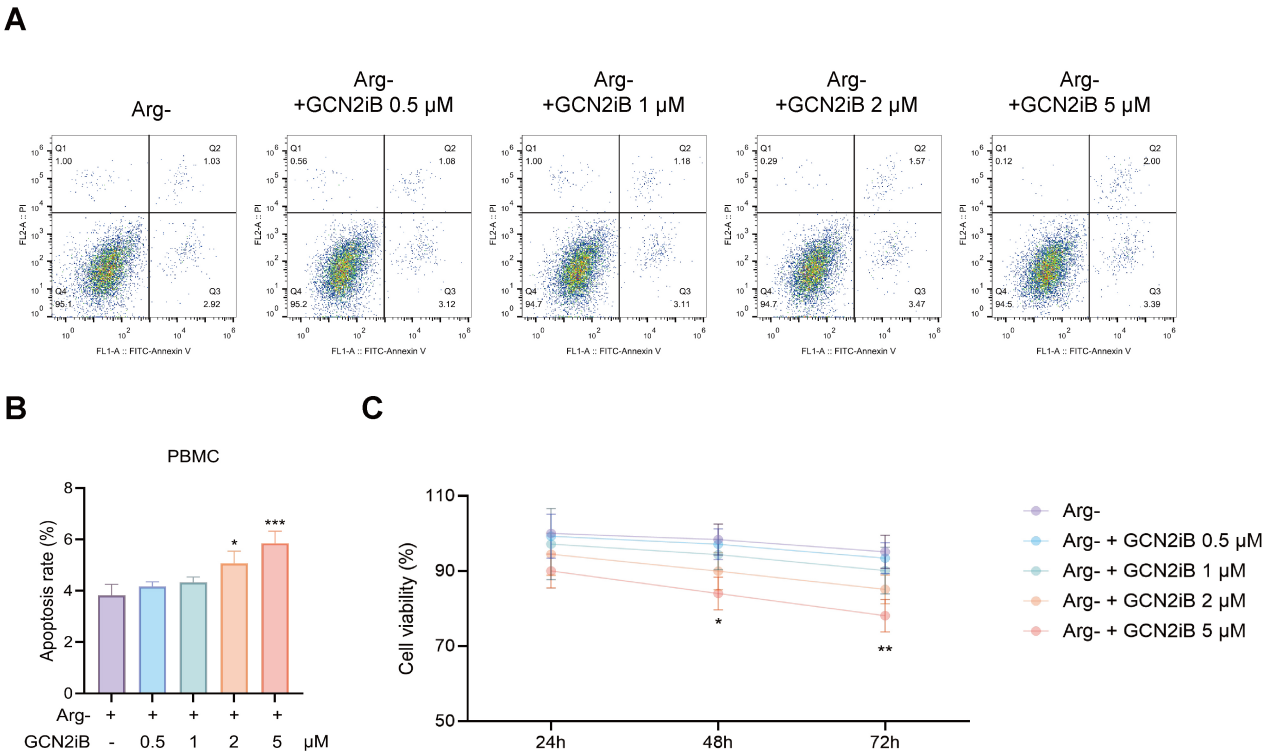

Fig. 6. GCN2 inhibition exhibits limited cytotoxicity in PBMCs under arginine deprivation. (A) Representative flow cytometry plots of apoptosis in PBMCs treated with increasing concentrations of GCN2iB (0.5, 1, 2, and 5 μM) under arginine-deprived conditions (Arg–) for 48 h. Apoptosis was assessed using Annexin V-FITC/PI staining. (B) Quantitative analysis of apoptotic cells (early + late apoptosis) in PBMCs based on flow cytometry data. (C) CCK-8 assay showing PBMC viability at 24 h, 48 h, and 72 h following treatment with increasing concentrations of GCN2iB under arginine deprivation. Relative metabolic activity is expressed as a percentage relative to the Arg– group at each time point. Data are presented as mean ± SD from three independent biological replicates. *$p < 0.05$, **$p < 0.01$, ***$p < 0.001$ vs. Arg– group.

with increasing concentrations of GCN2iB (0.5–5 μM) under arginine-deprived conditions. Flow cytometry analysis revealed a slight but dose-dependent increase in apoptosis, with the highest apoptotic rate observed at 5 μM GCN2iB, while the overall magnitude of apoptosis remained relatively low compared with that observed in MM cells (Fig. 6A,B, $p < 0.001$).

Consistently, CCK-8 assays showed that PBMC viability was only mildly affected by GCN2 inhibition, with a gradual decrease observed over time and at higher concentrations, but without pronounced cytotoxicity (Fig. 6C, $p < 0.001$). These findings suggest that GCN2 inhibition exerts limited effects on normal immune cell viability, highlighting a degree of relative selectivity toward tumor cells.

Discussion

In this study, we demonstrate that amino acid deprivation robustly activates the GCN2–eIF2α–ATF4 signaling axis in RPMI-8226 multiple myeloma cells, which promotes cell survival and enhances PD-L1 expression. Both physiological deprivation (arginine-free medium) and pharmacologic mimicry (halofuginone) induced GCN2 phosphorylation and downstream activation of ATF4 and CHOP, whereas GCN2 inhibition via GCN2iB reversed these effects. These findings highlight GCN2 as a critical metabolic stress sensor that supports RPMI-8226 myeloma cell adaptation and immune evasion. Notably, the apparent increase in CCK-8–based viability under arginine deprivation likely reflects enhanced metabolic adaptation rather than a true increase in cell proliferation. Under nutrient stress conditions, activation of the GCN2-mediated integrated stress response promotes ATF4-dependent adaptive programs that support T-cell survival, indicating that MM cells adapt to amino acid limitation rather than proliferate normally [17]. Our data are consistent with recent studies reporting that GCN2 serves as a master regulator of the ISR and promotes tumor cell survival under nutrient-deprived conditions [13,18]. Mechanistically, we found that GCN2 activation promotes survival by increasing Bcl-2 and decreasing Bax expression, consistent with previous reports showing that ATF4–CHOP signaling can rewire the apoptotic threshold in stressed cells [7,19]. Moreover, flow cytometry and Western blot analyses confirmed that

GCN2 inhibition increased Annexin V^+ apoptotic populations and reversed the survival advantage conferred by amino acid deprivation. These observations suggest that GCN2 functions as a metabolic stress sensor and molecular switch integrating amino acid deprivation signals with downstream stress pathways. Under nutrient stress such as glutamine or methionine starvation, GCN2 activates the ISR, leading to ATF4-mediated upregulation of TRAIL-R2 and caspase-8-dependent apoptosis [20]. Conversely, in immune-regulatory contexts, GCN2 promotes tolerance by enhancing IL-10 production and suppressing IL-12 translation in macrophages, thereby preventing inflammatory T-cell responses to apoptotic cells [21]. In retinoblastoma cells, GCN2 signaling also regulates survival and death by coordinating autophagy, G2 arrest, and apoptosis upon arginine deprivation, partly through modulation of SLC7A11 and mTORC1 activity [22]. Thus, GCN2 can either promote apoptosis or support adaptation depending on the cellular context, consistent with our findings that it confers a survival advantage in MM.

A particularly novel finding of the present study is the association between GCN2 signaling and PD-L1 regulation in MM cells. We found that PD-L1 expression at both the mRNA and protein levels was significantly upregulated by arginine deprivation and halofuginone, and this effect was partially reversed by GCN2iB. Flow cytometry further validated these findings by showing an increased percentage of $CD38^+PD\text{-}L1^+$ MM cells under stress, consistent with enhanced immune-evasive potential. While previous studies have implicated metabolic stress in promoting PD-L1 via the PERK pathway [7], our results support a distinct mechanism in which GCN2–ATF4 contributes to immunomodulatory gene expression, in agreement with observations in other cancers and immune cell systems [23,24]. From a translational perspective, these findings suggest that GCN2 inhibition may provide a dual therapeutic benefit in MM by simultaneously impairing metabolic adaptation and reducing PD-L1–mediated immune escape, in line with the growing interest in combining immunotherapy with metabolic stress modulation.

However, several limitations should be acknowledged in this study. First, this study is limited to a single MM cell line (RPMI-8226), and therefore may not fully capture the heterogeneity of multiple myeloma. Validation in additional MM cell lines and primary patient-derived cells will be required to confirm the generalizability of these findings. Second, although we focused on PD-L1, other immune modulators (e.g., IDO2, Galectin-9) may also be influenced by GCN2 and warrant further investigation. Lastly, the long-term impact of GCN2 blockade on immune cell subsets in the bone marrow niche remains to be clarified.

Conclusion

This study demonstrates that activation of GCN2 promotes survival and PD-L1 expression in RPMI-8226 multiple myeloma cells under amino acid deprivation, thereby supporting both metabolic adaptation and immune evasion. Conversely, pharmacological inhibition of GCN2 reverses these effects, suggesting that targeting this pathway may represent a promising therapeutic strategy for multiple myeloma.

Availability of Data and Materials

The data used and analyzed during the current study are available from the corresponding author upon reasonable request.

Author Contributions

JP, YQJ and LNZ conceived and designed the study. JP and LNZ conducted the study. LNZ contributed to data acquisition. JP analyzed the data. YQJ interpreted the data. JP, YQJ and LNZ edited the manuscript draft. All authors have been involved in revising it critically for important intellectual content. All authors gave final approval of the version to be published. All authors have participated sufficiently in the work to take public responsibility for appropriate portions of the content and agreed to be accountable for all aspects of the work in ensuring that questions related to its accuracy or integrity.

Ethics Approval and Consent to Participate

Not applicable.

Acknowledgment

Not applicable.

Funding

Not applicable.

Conflict of Interest

The authors declare no conflict of interest.

References

[1] Vrtis MC. Multiple Myeloma. Home Healthcare now. 2024; 42: 140–149. https://doi.org/10.1097/NHH.0000000000001249

[2] Brigle K, Rogers B. Pathobiology and Diagnosis of Multiple Myeloma. Seminars in Oncology Nursing. 2017; 33: 225–236. https://doi.org/10.1016/j.soncn.2017.05.012

[3] Lombardi AF, Wong JH, High R, Ma Y, Jerban S, Tang Q, et al. AcidoCEST MRI Evaluates the Bone Microenvironment in Multiple Myeloma. Molecular Imaging and Biology. 2021; 23: 865–873. https://doi.org/10.1007/s11307-021-01611-2

[4] Falcón P, Brito Á, Escandón M, Roa JF, Martínez NW, Tapia-Godoy A, et al. GCN2-Mediated eIF2α Phosphorylation Is Required for Central Nervous System Remyelination. International Journal of Molecular Sciences. 2025; 26: 1626. https://doi.org/10.3390/ijms26041626

[5] Collier AE, Wek RC, Spandau DF. Human Keratinocyte Differentiation Requires Translational Control by the eIF2α Kinase GCN2. The Journal of Investigative Dermatology. 2017; 137: 1924–1934. https://doi.org/10.1016/j.jid.2017.04.029

[6] Spaulding EL, Hines TJ, Bais P, Tadenev ALD, Schneider R, Jewett D, et al. The integrated stress response contributes to tRNA synthetase-associated peripheral neuropathy. Science (New York, N.Y.). 2021; 373: 1156–1161. https://doi.org/10.1126/science.abb3414

[7] Rozpedek W, Pytel D, Mucha B, Leszczynska H, Diehl JA, Majsterek I. The Role of the PERK/eIF2α/ATF4/CHOP Signaling Pathway in Tumor Progression During Endoplasmic Reticulum Stress. Current Molecular Medicine. 2016; 16: 533–544. https://doi.org/10.2174/1566524016666160523143937

[8] Waad Sadiq Z, Brioli A, Al-Abdulla R, Çetin G, Schütt J, Murua Escobar H, et al. Immunogenic cell death triggered by impaired deubiquitination in multiple myeloma relies on dysregulated type I interferon signaling. Frontiers in Immunology. 2023; 14: 982720. https://doi.org/10.3389/fimmu.2023.982720

[9] Yang M, Cao M, Zhang X, Fu B, Chen Y, Tan Y, et al. IDO1 inhibitors are synergistic with CXCL10 agonists in inhibiting colon cancer growth. Biomedicine & Pharmacotherapy = Biomedecine & Pharmacotherapie. 2024; 179: 117412. https://doi.org/10.1016/j.biopha.2024.117412

[10] Oudaert I, Van der Vreken A, Maes A, De Bruyne E, De Veirman K, Vanderkerken K, et al. Metabolic cross-talk within the bone marrow milieu: focus on multiple myeloma. Experimental Hematology & Oncology. 2022; 11: 49. https://doi.org/10.1186/s40164-022-00303-z

[11] Schafer CC, Wang Y, Hough KP, Sawant A, Grant SC, Thannickal VJ, et al. Indoleamine 2,3-dioxygenase regulates anti-tumor immunity in lung cancer by metabolic reprogramming of immune cells in the tumor microenvironment. Oncotarget. 2016; 7: 75407–75424. https://doi.org/10.18632/oncotarget.12249

[12] Yan G, Han Z, Kwon Y, Jousma J, Nukala SB, Prosser BL, et al. Integrated Stress Response Potentiates Ponatinib-Induced Cardiotoxicity. Circulation Research. 2024; 134: 482–501. https://doi.org/10.1161/CIRCRESAHA.123.323683

[13] Szaruga M, Janssen DA, de Miguel C, Hodgson G, Fatalska A, Pitera AP, et al. Activation of the integrated stress response by inhibitors of its kinases. Nature Communications. 2023; 14: 5535. https://doi.org/10.1038/s41467-023-40823-8

[14] Keller TL, Zocco D, Sundrud MS, Hendrick M, Edenius M, Yum J, et al. Halofuginone and other febrifugine derivatives inhibit prolyl-tRNA synthetase. Nature Chemical Biology. 2012; 8: 311–317. https://doi.org/10.1038/nchembio.790

[15] Xu S, Liu Z, Tian T, Zhao W, Wang Z, Liu M, et al. The clinical antiprotozoal drug halofuginone promotes weight loss by elevating GDF15 and FGF21. Science Advances. 2025; 11: eadt3142. https://doi.org/10.1126/sciadv.adt3142

[16] Kocik-Krol J, Stec M, Siedlar M, Vo TH, Rani S, Skalniak L. A PD-1/PD-L1-Sensitive Co-culture-Based Primary T-Cell Activation Assay. Methods in Molecular Biology (Clifton, N.J.). 2026; 2959: 85–95. https://doi.org/10.1007/978-1-0716-4734-9_6

[17] Carlson KR, Georgiadis MM, Tameire F, Staschke KA, Wek RC. Activation of Gcn2 by small molecules designed to be inhibitors. The Journal of Biological Chemistry. 2023; 299: 104595. https://doi.org/10.1016/j.jbc.2023.104595

[18] Lu HJ, Koju N, Sheng R. Mammalian integrated stress responses in stressed organelles and their functions. Acta Pharmacologica Sinica. 2024; 45: 1095–1114. https://doi.org/10.1038/s41401-023-01225-0

[19] Coker-Gurkan A, Can E, Sahin S, Obakan-Yerlikaya P, Arisan ED. Atiprimod triggered apoptotic cell death via acting on PERK/eIF2α/ATF4/CHOP and STAT3/NF-KB axis in MDA-MB-231 and MDA-MB-468 breast cancer cells. Molecular Biology Reports. 2021; 48: 5233–5247. https://doi.org/10.1007/s11033-021-06528-1

[20] Yerbes R, Mora-Molina R, Fernández-Farrán FJ, Hiraldo L, López-Rivas A, Palacios C. Limiting glutamine utilization activates a GCN2/TRAIL-R2/Caspase-8 apoptotic pathway in glutamine-addicted tumor cells. Cell Death & Disease. 2022; 13: 906. https://doi.org/10.1038/s41419-022-05346-y

[21] Ravishankar B, Liu H, Shinde R, Chaudhary K, Xiao W, Bradley J, et al. The amino acid sensor GCN2 inhibits inflammatory responses to apoptotic cells promoting tolerance and suppressing systemic autoimmunity. Proceedings of the National Academy of Sciences of the United States of America. 2015; 112: 10774–10779. https://doi.org/10.1073/pnas.1504276112

[22] Wang D, Chu WK, Yam JCS, Pang CP, Leung YC, Shum ASW, et al. GCN2-SLC7A11 axis coordinates autophagy, cell cycle and apoptosis and regulates cell growth in retinoblastoma upon arginine deprivation. Cancer & Metabolism. 2024; 12: 31. https://doi.org/10.1186/s40170-024-00361-3

[23] Liu D, Glubb D, O'Mara T, Ford CE. The Multi-Kinase Inhibitor GZD824 (Olverembatinib) Shows Pre-Clinical Efficacy in Endometrial Cancer. Cancer Medicine. 2025; 14: e70531. https://doi.org/10.1002/cam4.70531

[24] Manchon E, Hirt N, Versier B, Soundiramourty A, Juricek L, Lebbe C, et al. Harnessing nutrient scarcity for enhanced CAR-T-cell potency and safety in solid tumors. Cellular & Molecular Immunology. 2025; 22: 645–660. https://doi.org/10.1038/s41423-025-01290-x